C/EBP homologous protein inhibits tissue repair in response to gut injury and is inversely regulated with chronic inflammation

N Waldschmitt[1,2], E Berger[1], E Rath[1], RB Sartor[3], B Weigmann[4], M Heikenwalder[5], M Gerhard[6], K-P Janssen[7] and D Haller[1,2]

Loss of intestinal epithelial cell (IEC) homeostasis and apoptosis negatively affect intestinal barrier function. Uncontrolled activation of the unfolded protein response (UPR) in IEC contributes to an impaired barrier and is implicated in the pathogenesis of inflammatory bowel diseases. However, the contribution of the UPR target gene C/EBP homologous protein (CHOP), an apoptosis-associated transcription factor, to inflammation-related disease susceptibility remains unclear. Consistent with observations in patients with ulcerative colitis, we show that despite UPR activation in the epithelium, CHOP expression was reduced in mouse models of T-cell-mediated and bacteria-driven colitis. To elucidate the molecular mechanisms of IEC-specific CHOP expression, we generated a conditional transgenic mouse model (*Chop*$^{IEC\ Tg/Tg}$). Chop overexpression increased the susceptibility toward dextran sodium sulfate (DSS)-induced intestinal inflammation and mucosal tissue injury. Furthermore, a delayed recovery from DSS-induced colitis and impaired closure of mechanically induced mucosal wounds was observed. Interestingly, these findings seemed to be independent of CHOP-mediated apoptosis. *In vitro* and *in vivo* cell cycle analyses rather indicated a role for CHOP in epithelial cell proliferation. In conclusion, these data show that IEC-specific overexpression impairs epithelial cell proliferation and mucosal tissue regeneration, suggesting an important role for CHOP beyond mediating apoptosis.

INTRODUCTION

Inflammatory bowel diseases (IBD), including Crohn's disease and ulcerative colitis (UC), are chronically relapsing, immune-mediated disorders of still unknown etiology. Genome-wide association studies in IBD patients identified genetic risk loci related to the loss of intestinal epithelial cell (IEC) homeostasis.[1–4] Genetic predispositions increasing susceptibility to chronic inflammation affect innate immune mechanisms and cellular stress responses relevant for intestinal barrier function and microbial defense. Unfolded protein responses (UPR) of the endoplasmic reticulum (ER) and mitochondria represent cellular stress responses known to be involved in the pathogenesis of intestinal inflammation. Induction of UPR-related mechanisms is associated with changes in intestinal permeability, epithelial regeneration, or apoptosis as well as alterations in synthesis and secretion of antimicrobial substances.[5–8]

One of the transcription factors strongly involved in UPR-related cell death is C/EBP homologous protein (CHOP), also called GADD153 (growth arrest- and DNA damage-inducible gene 153).[9] CHOP belongs to the family of bZIP transcription factors and is expressed at low levels under physiological conditions.[10] The expression of CHOP is tightly regulated on both posttranscriptional and posttranslational levels. Upon stress, such as hypoxia, nutrient deprivation, and protein misfolding or malfolding in the ER and mitochondria, CHOP levels increase.[11–15] The transcriptional activation of CHOP

[1]Chair of Nutrition and Immunology, Technische Universität München, Freising, Germany. [2]ZIEL—Research Center for Nutrition and Food Sciences, Biofunctionality Unit, Technische Universität München, Freising, Germany. [3]Center for Gastrointestinal Biology and Disease, University of North Carolina, Chapel Hill, North Carolina, USA. [4]First Medical Clinic, University of Erlangen, Erlangen, Germany. [5]Institute of Virology, Technische Universität München/Helmholtz Zentrum Munich, Munich, Germany. [6]Institute of Medical Microbiology, Immunology and Hygiene, Technische Universität München, Munich, Germany and [7]Department of Surgery, Klinikum rechts der Isar, Technische Universität München, Munich, Germany. Correspondence: D Haller (dirk.haller@tum.de)

Received 6 November 2013; accepted 6 April 2014; advance online publication 21 May 2014. doi:10.1038/mi.2014.34

protein is further dependent on stress-induced protein phosphorylation and heterodimer formation.[10,16–20] Dimerization with CHOP protein attenuates the binding capacity of most binding partners to specific DNA sequences; however, unique DNA recognition sites are activated, which cause the expression of so-called downstream target genes of CHOP.[21] Among those are genes such as *Bcl-2*, *Atf3*, *Trb3*, *Ero1α*, *Gadd34*, and *Bim*, known to promote pro-apoptotic signaling.[22–26] In line, CHOP knockout mice show reduced intestinal apoptosis in response to experimental colitis.[27] Interestingly, studies in UC patients indicate that both CHOP mRNA and protein expression is significantly decreased,[28] even though ER UPR and mitochondria UPR were shown to be activated under inflammatory conditions.[8,27]

Accordingly, we observed downregulation of CHOP mRNA and protein expression in different animal models of colitis. To elucidate the possible effects of the selective downregulation of CHOP under inflammatory conditions and to investigate the functional consequences of sustained CHOP protein expression in a tissue-specific resolution, we generated *Chop*$^{\text{IEC Tg/Tg}}$ mice that express high levels of CHOP protein restricted to the IEC layer.

RESULTS

CHOP mRNA and protein expression is reduced in IECs under chronic inflammatory conditions

Previous studies with UC patients have shown that both CHOP mRNA and protein expression is downregulated in colonic tissue under inflammatory conditions.[28] We obtained similar results analyzing CHOP mRNA and protein expression in IEC isolates derived from mouse models of T-cell-mediated and bacteria-driven chronic colitis. In the adoptive transfer model of colitis (Rag2$^{-/-}$ and Rag2$^{-/-}$ × IL-10$^{-/-}$), the downregulation of CHOP in IECs was evident 4 weeks after the transfer of colitogenic T cells derived from wild-type (WT) and IL-10$^{-/-}$ donor mice (**Figure 1a–c**). Similar results were shown after mono- or dual-association of germ-free IL-10$^{-/-}$ mice with *Enterococcus faecalis* and/or *Escherichia coli* for 16 weeks (**Figure 1d**). The reduction of CHOP mRNA and protein expression was found to be highly associated with increasing histopathological scores. At the same time, the expression of the ER UPR-marker glucose-regulated protein 78 (GRP78) was induced, indicating a dissociation between UPR activation and CHOP expression in chronic intestinal inflammation. To further investigate the functional role of CHOP protein in the intestinal epithelium, we generated the mouse model *Chop*$^{\text{IEC Tg/Tg}}$ that expresses high levels of CHOP restricted to IECs.

Chop$^{\text{IEC Tg/Tg}}$ mice do not spontaneously develop an inflammatory disease phenotype

Chop$^{\text{IEC Tg/Tg}}$ mice were generated as mentioned in Materials and methods (**Figure 2a**). The IEC-restricted overexpression of hemagglutinin (HA)-tagged CHOP was shown on mRNA level in laser-microdissected cells derived from the intestinal epithelium, lamina propria, and muscularis of *Chop*$^{\text{IEC Tg/Tg}}$ mice and WT controls (**Figure 2b**). *Chop*$^{\text{IEC Tg/Tg}}$ mice also exhibit high expression of CHOP mRNA and protein in isolated IECs derived from the small and large intestine (**Figure 2c**; see **Supplementary Figure S1** online). The average induction of CHOP mRNA was around 30-fold than that of WT controls. Both anti-HA and anti-CHOP antibodies were used for western blotting analyses to confirm the expression of transgenic CHOP protein. Bands obtained by anti-CHOP and anti-HA antibodies, respectively, indicated a shift in molecular weight from ~26 to ~30 kDa, suggesting posttranslational modifications. To ensure the capability of the transgenic protein to act as transcription factor, the nuclear localization of CHOP-HA was demonstrated by immunflouresence staining using anti-HA antibody (**Figure 2d**). Yet, *Chop*$^{\text{IEC Tg/Tg}}$ mice do not develop any spontaneous phenotype in the intestine, and epithelial morphology of transgenic mice at different ages appeared comparable to WT controls with respect to villus height, crypt depth, and mucus area (**Figure 3**; see **Supplementary Figure S2**). Despite the fact that IECs overexpress an apoptosis-associated protein, the numbers of both cleaved caspase 3 (cC3)- and Ki-67-positive IECs remained unaltered, indicating neither enhanced apoptosis nor changes in proliferation (**Figure 3b–d** and see **Supplementary Figure S2**).

IEC-specific overexpression of CHOP protein aggravates dextran sodium sulfate (DSS)-induced colitis

To examine the impact of IEC-restricted CHOP overexpression in a chemically induced colitis model, we applied three different DSS protocols. 2% DSS was orally administered for 3 and 7 days to examine early and late acute effects. Additionally, 2% DSS was given for 5 days followed by 5 days of normal drinking water to investigate intestinal recovery. At all the investigated time points, transgenic mice were more susceptible to DSS-induced mucosal injury, as reflected by significantly increased histological scores (**Figure 4a,b**; **Table 1**), body weight decrease, and elevated Disease Activity Index (see **Supplementary Figure S3 A, B**). After 3 days of DSS treatment, the more severe effect seen in *Chop*$^{\text{IEC Tg/Tg}}$ mice was accompanied by the increased numbers of infiltrating macrophages and antigen-presenting cells, but not B or T cells (**Figure 4c–f**). In this early acute phase of inflammation, also the numbers of cC3-positive (apoptotic) IECs were elevated when compared with DSS-treated WT mice (**Figure 5a,b**). Interestingly, the dissociation of UPR activation and reduced CHOP expression demonstrated in the models of chronic intestinal inflammation (**Figure 1c,d**) was confirmed in WT mice suffering from acute DSS-induced colitis after 3 and 7 days of treatment (**Figure 5c**; see **Supplementary Figure S3C**). In contrast, during the recovery phase after DSS treatment, CHOP protein levels seemed to be unchanged while GRP78 expression decreased (**Figure 5e**). None of the three applied DSS protocols had an impact on the CAG promoter-driven transgene expression in *Chop*$^{\text{IEC Tg/Tg}}$ mice (**Figure 5c,e**; see **Supplementary Figure S3C**). In contrast to CHOP protein, mRNA levels of *Gadd34* and *Ero1α*, genes belonging to the group of

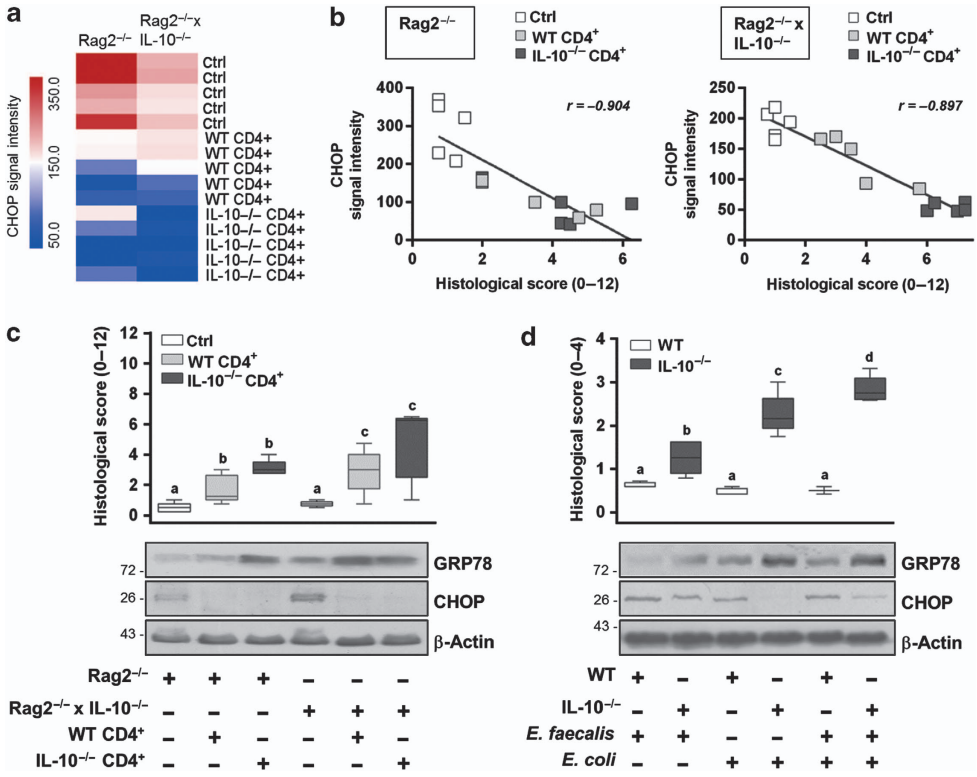

Figure 1 IEC-specific downregulation of C/EBP homologous protein (CHOP) mRNA and protein expression in mouse models of chronic colitis. (**a**) Gene expression profiling was performed by using large intestinal intestinal epithelial cell (IEC) isolates from untreated controls (ctrl) as well as Rag2$^{-/-}$ and Rag2$^{-/-}$ × IL-10$^{-/-}$ mice 4 weeks after adoptive transfer of wild-type CD4^{+} (WT CD4^{+}) and IL-10$^{-/-}$ CD4^{+} T cells ($n=5$). Signal intensity of CHOP probes indicates reduced CHOP mRNA expression in response to adoptive T-cell transfer. (**b**) Signal intensity of CHOP probes indicates a significant negative correlation of CHOP mRNA expression and histological score according to Spearman's rank correlation. (**c**, **d**) Glucose-regulated protein 78 (GRP78) and CHOP expression of pooled large intestinal IEC isolates analyzed by western blotting. β-Actin served as a loading control. Box plots: mean histopathological score ± s.d. Data sets were analyzed by two-way ANOVA with genotype and treatment as main factors followed by multiple comparison procedure by Holm–Sidak method. (**c**) Rag2$^{-/-}$ and Rag2$^{-/-}$ × IL-10$^{-/-}$ mice 4 weeks after adoptive transfer of WT CD4^{+} and IL-10$^{-/-}$ CD4^{+} T cells ($n=5$). (**d**) Germ-free IL-10$^{-/-}$ mice and WT controls were associated with colitogenic *E. faecalis* and/or *E. coli* for 16 weeks ($n=5$).

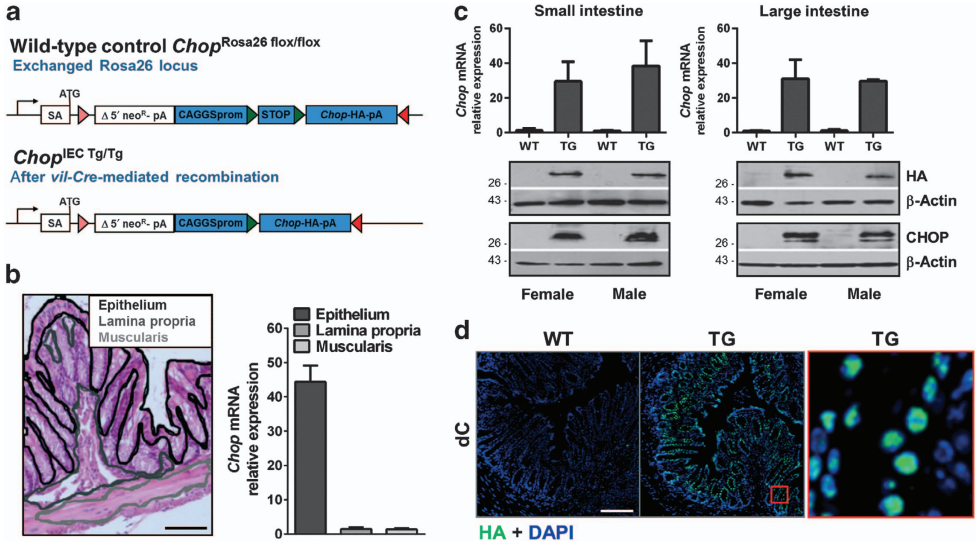

Figure 2 Generation of new mouse model *Chop*$^{IEC\ Tg/Tg}$. (**a**) *Chop*$^{Rosa26\ flox/flox}$ mice were mated with *Vil-cre*-positive mice resulting in high expression of hemagglutinin (HA)-tagged C/EBP homologous protein (CHOP). (**b**) CHOP mRNA expression was assessed using isolates of microdissected cells derived from the intestinal epithelium, lamina propria, and muscularis of *Chop*$^{IEC\ Tg/Tg}$ mice and wild-type (WT) controls. Bar = 100 μm ($n=3$). (**c**) Intestinal epithelial cell isolates from small and large intestine of *Chop*$^{IEC\ Tg/Tg}$ mice and WT controls ($n=3$) were examined for transgene expression by quantitativePCR and western blotting using primary antibodies against CHOP and HA. Anti-β-Actin antibody was used as loading control. (**d**) Immunofluorescence staining was performed on colonic tissue sections applying anti-HA antibody. 4,6-Diamidino-2-phenylindole (DAPI) was used for nuclear counterstain. dC, distal colon.

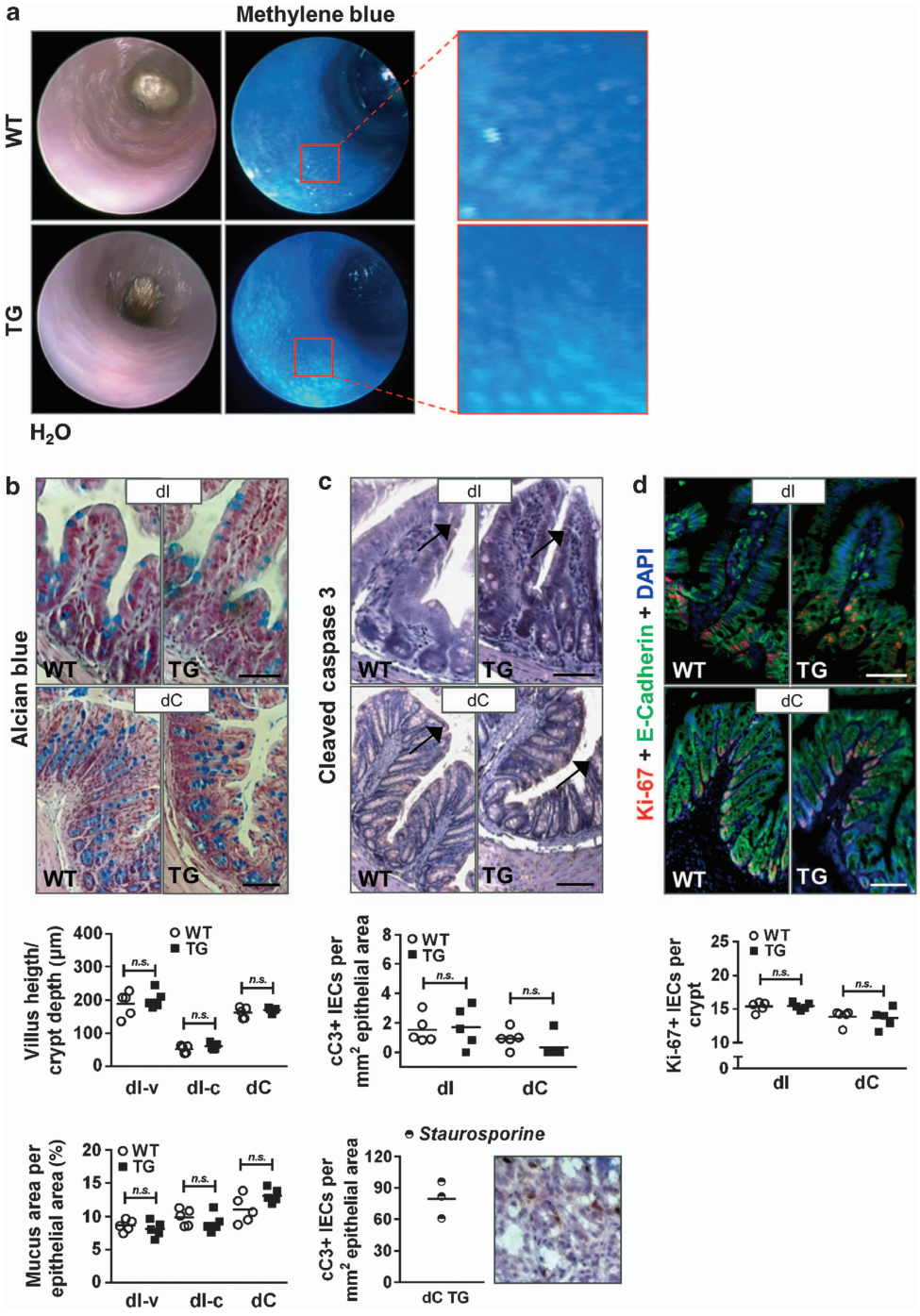

Figure 3 *Chop*$^{IEC\ Tg/Tg}$ mice do not spontaneously develop an inflammatory phenotype. (**a**) Colonoscopy was performed on transgenic (TG) mice and wild-type (WT) controls before and after staining of the intestinal epithelium with methylene blue. (**b**) Tissue sections of distal ileum (dI) and distal colon (dC) from *Chop*$^{IEC\ Tg/Tg}$ mice and WT controls were stained with alcian blue ($n=5$). Villus height, crypt depth, total epithelial area, and mucus area were measured, and means were calculated. Mucus area is given as a percentage of total epithelial area. (**c**) Caspase 3 cleavage was analyzed by immunohistochemistry. The numbers of apoptotic cells were assessed by counting cC3-positive epithelial cells in a total epithelial area of 1 mm^2 (arrows). Positive control staining was performed using distal colon from *Chop*$^{IEC\ Tg/Tg}$ mice that was incubated *ex vivo* with 1 µM staurosporine for 2 h at 37 °C. (**d**) The numbers of proliferating cells were determined by applying anti-Ki-67 antibody on tissue sections of dI and dC from TG mice and WT controls ($n=5$). Means were calculated as the numbers of proliferating cells per crypt. Scale bars for all tissue sections represent 50 µm (dI) and 100 µm (dC). All data sets were analyzed by non-parametric rank-sum test, $P<0.05$, $P<0.01$, and $P<0.001$ were considered statistically significant. NS, not significant.

downstream target genes of CHOP, were significantly upregulated in the 3 days of DSS treatment groups. The induction of *Gadd34* and *Ero1α* was more pronounced in *Chop*$^{IEC\ Tg/Tg}$ mice (**Figure 5d**). Yet, the difference in *Gadd34* and *Ero1α* expression between WT and transgenic mice was not observed in the recovery phase (**Figure 5f**).

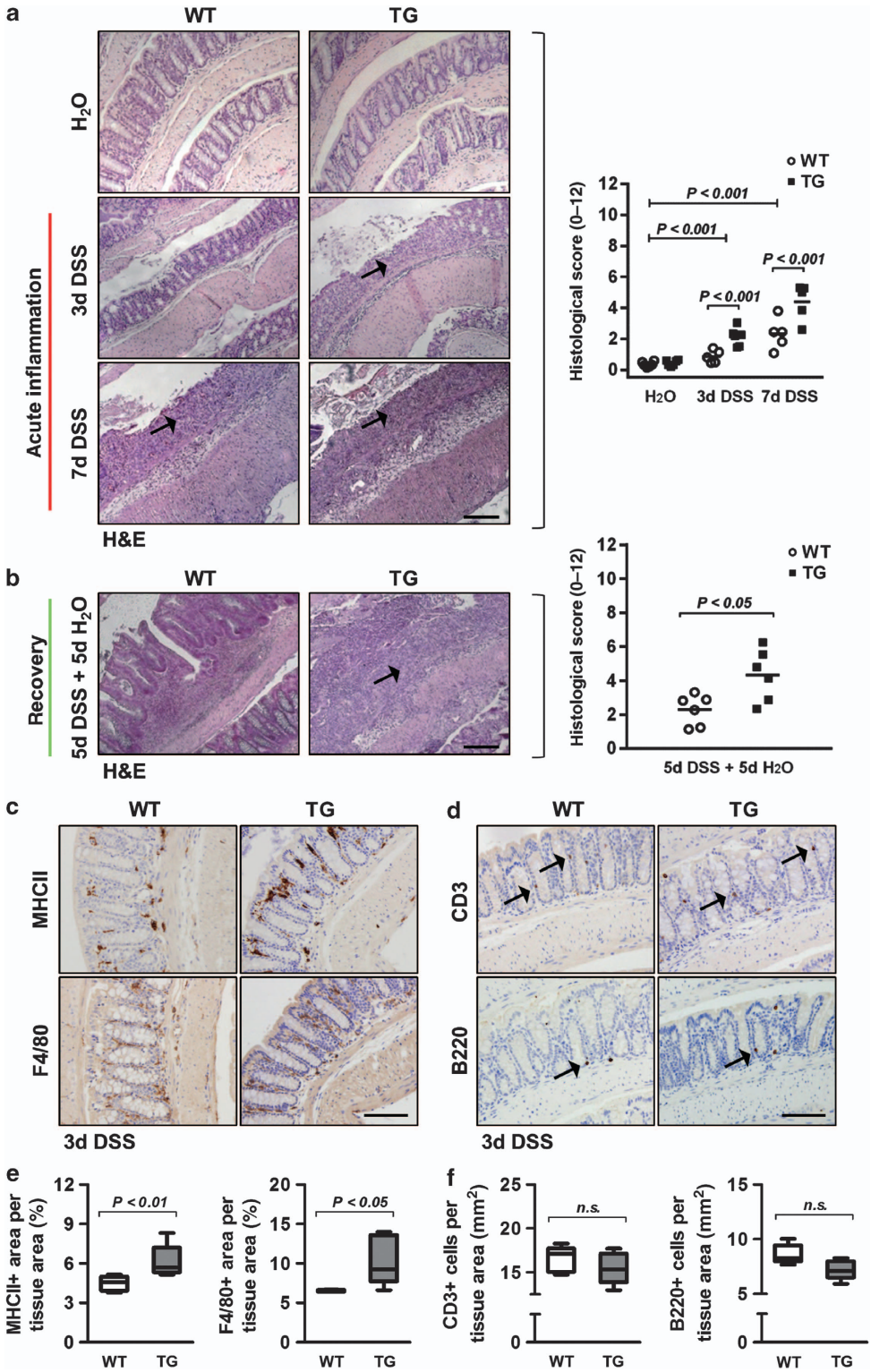

Figure 4 *Chop*$^{IEC\ Tg/Tg}$ mice are more susceptible to dextran sodium sulfate (DSS)-induced colitis. (**a**) Transgenic (TG) mice and wild-type (WT) controls ($n = 5$–6) were orally administered water and 2% of DSS for 3 and 7 days, respectively. Histological scores of colon tissue sections from DSS-treated and water-treated mice were blindly assessed. Bar = 200 μm. Data sets of water-treated as well as 3d and 7d DSS-treated mice were analyzed by two-way ANOVA with genotype and DSS treatment as main factors followed by multiple comparison procedure by Holm–Sidak method, $P < 0.05$, $P < 0.01$, and $P < 0.001$ were considered statistically significant. (**b**) Mice ($n = 6$) were given 2% DSS for 5 days followed by a period of 5 days for recovery. Histological scores of colon sections from DSS-treated and water-treated mice were blindly assessed. Bar = 200 μm. Statistical significance of data sets from mice in recovery was evaluated by non-parametric rank-sum test. $P < 0.05$, $P < 0.01$, and $P < 0.001$ were considered statistically significant. Arrows indicate DSS-induced mucosal tissue damage. (**c**–**f**) The numbers of infiltrating MHCII + antigen-presenting cells, F4/80 + macrophages, CD3 + T cells, and B220 + B cells were determined by applying the respective antibody on tissue sections of dC from TG mice and WT controls ($n = 5$). Bar = 100 μm. All data sets were analyzed by non-parametric rank-sum test, $P < 0.05$ and $P < 0.01$ were considered statistically significant. NS, not significant.

Table 1 Histological evaluation of DSS experiments: 3d 2% DSS, 7d 2% DSS, and 5d 2% DSS + 5d H_2O

Treatment	Group	Changes in intestinal architecture and epithelial damage (0–6)	Genotype	Within H_2O	Within DSS	Treatment	Within WT	Within TG
H_2O	WT	0.275 ± 0.175	Data sets H_2O, 3d 2% DSS, and 7d 2% DSS were analyzed by TWA with genotype and DSS treatment as main factors					
	TG	0.283 ± 0.157						
3d 2% DSS	WT	0.510 ± 0.224	***	NS	***	***	NS	***
	TG	1.331 ± 0.357						
7d 2% DSS	WT	1.375 ± 0.587	**	NS	***	***	**	***
	TG	2.824 ± 0.774						
5d 2% DSS + 5d H_2O	WT	1.092 ± 0.403	Data of 5d 2% DSS + 5d H_2O were analyzed by Student's *t*-test					
	TG	2.450 ± 0.913	—	—	—	**	—	—

Treatment	Group	Infiltration with inflammatory cells (0–6)	Genotype	Within H_2O	Within DSS	Treatment	Within WT	Within TG
H_2O	WT	0.075 ± 0.063	Data sets H_2O, 3d 2% DSS, and 7d 2% DSS were analyzed by TWA with genotype and DSS treatment as main factors					
	TG	0.150 ± 0.063						
3d 2% DSS	WT	0.385 ± 0.234	**	NS	**	***	*	***
	TG	0.788 ± 0.264						
7d 2% DSS	WT	0.945 ± 0.462	*	NS	**	***	***	***
	TG	1.580 ± 0.419						
5d 2% DSS + 5d H_2O	WT	1.202 ± 0.627	Data of 5d 2% DSS + 5d H_2O were analyzed by non-parametric rank-sum test					
	TG	1.879 ± 0.623	—	—	—	NS	—	—

Treatment	Group	Histological score (0–12)	Genotype	Within H_2O	Within DSS	Treatment	Within WT	Within TG
H_2O	WT	0.350 ± 0.170	Data sets H_2O, 3d 2% DSS, and 7d 2% DSS were analyzed by TWA with genotype and DSS treatment as main factors					
	TG	0.433 ± 0.189						
3d 2% DSS	WT	0.895 ± 0.420	***	NS	***	***	*	***
	TG	2.119 ± 0.588						
7d 2% DSS	WT	2.320 ± 1.669	**	NS	***	***	***	***
	TG	4.404 ± 1.170						
5d 2% DSS + 5d H_2O	WT	2.294 ± 0.911	Data of 5d 2% DSS + 5d H_2O were analyzed by non-parametric rank-sum test					
	TG	4.329 ± 1.514	—	—	—	*	—	—

Abbreviations: DSS, dextran sodium sulfate; TG, transgenic; TWA, two-way ANOVA; WT, wild type.
Data sets H_2O, 3d 2% DSS, and 7d 2% DSS were analyzed by TWA with genotype and DSS treatment as main factors followed by multiple comparison procedure by Holm–Sidak method, $^*P<0.05$, $^{**}P<0.01$, and $^{***}P<0.001$ were considered statistically significant. Statistical significance of 5d 2% DSS + 5d H_2O was evaluated by non-parametric rank-sum test, $^*P<0.05$, $^{**}P<0.01$, and $^{***}P<0.001$ were considered statistically significant.

As the differences observed between WT and *Chop*$^{\text{IEC Tg/Tg}}$ mice regarding cC3-positive IECs were quite small considering the overall induction comparing the DSS-treated and water control groups (**Figures 3c** and **5a,b**), it seemed unlikely that enhanced apoptosis was causative for the more pronounced epithelial damage. Furthermore, the results obtained by the DSS recovery experiment could also hint toward a delayed wound closure/healing process.

Mucosal tissue regeneration is impaired in *Chop*$^{\text{IEC Tg/Tg}}$ mice after mechanical injury

Regeneration of the intestinal epithelium is one of the most important properties required for maintaining epithelial integrity, in particular under conditions of acute and chronic inflammation.[29] Concluding the results from the chemically (DSS)-induced colitis, we next sought to investigate intestinal wound healing in a more specific approach. To determine whether healing was impaired in disease-free *Chop*$^{\text{IEC Tg/Tg}}$ mice compared with WT mice, mucosal wounds were mechanically induced in the colon using biopsy clamps. Wound closure was monitored by video colonoscopy on days 0, 1, 2, 3 and 5 after wound induction, and wound diameters as the percentage of initial wound size were calculated (**Figure 6a,b**). In transgenic mice, wound closure was significantly delayed from day 2 onwards, whereby 3 out of the 6 animals were sampled after colonoscopic inspection on day 3 for further

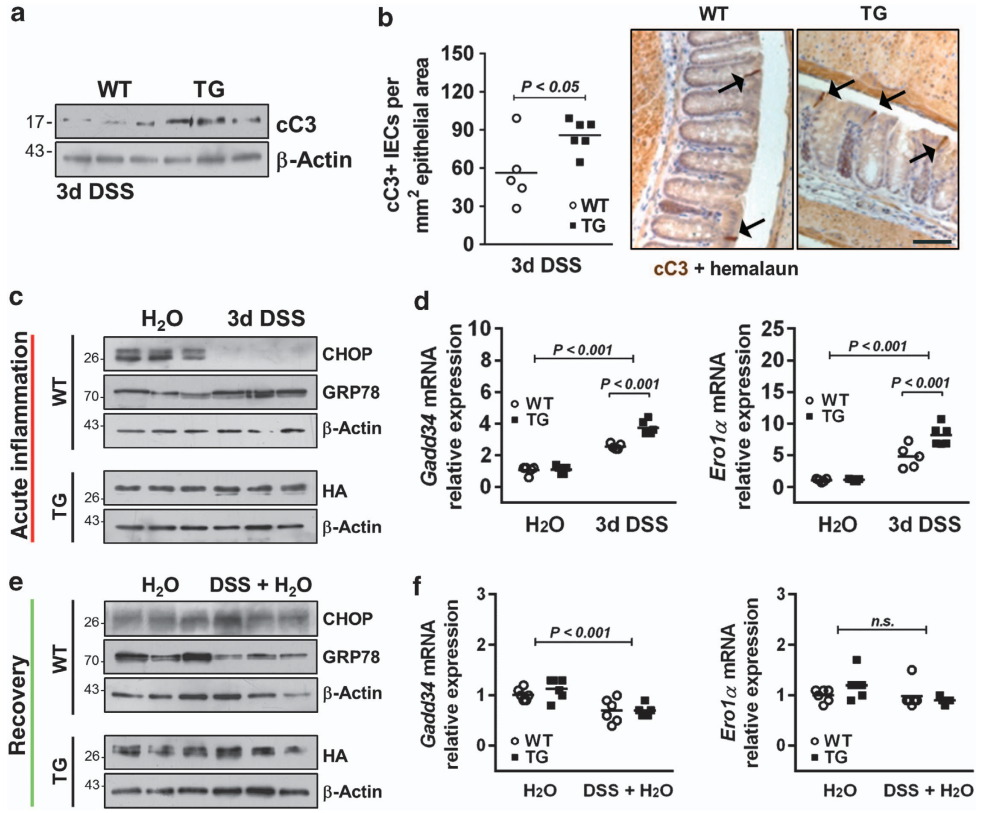

Figure 5 C/EBP homologous protein (CHOP) expression is regulated independently of unfolded protein response signaling. (**a**, **c**) Intestinal epithelial cells (IECs) were isolated from water-treated and 3d dextran sodium sulfate (DSS)-treated mice. (**a**, **b**) Caspase 3 cleavage determined by western blotting analysis (**a**) and immunohistochemistry (**b**). Arrows indicate cC3-positive IECs. The number of apoptotic cells were assessed by counting cC3-positive epithelial cells ($n = 5$). Bar = 100 μm. Statistical significance was evaluated by non-parametric rank-sum test. $P < 0.05$ was considered statistically significant. (**c**) Western blotting analysis was performed by using antibodies against CHOP, glucose-regulated protein 78 (GRP78) and HA tag; anti-β-actin antibody was used as a loading control. (**d**) Expression of CHOP target genes *Ero1α* and *Gadd34* was analyzed by quantitative PCR (qPCR). Data sets were analyzed by two-way ANOVA (TWA) with genotype and DSS treatment as main factors followed by multiple comparison procedure by Holm–Sidak method, $P < 0.05$, $P < 0.01$, and $P < 0.001$ were considered statistically significant. (**e**) Colonic IECs were isolated from 5d DSS-treated transgenic (TG) mice and wild-type (WT) controls after a period of 5 days for recovery. Western blotting on IEC lysates was performed using anti-CHOP, anti-GRP78, anti-HA, and anti-β-actin antibodies. (**f**) mRNA expression of Gadd34 and Ero1α was analyzed by qPCR. Data sets were analyzed by TWA with genotype and DSS treatment as main factors followed by multiple comparison procedure by Holm–Sidak method, $P < 0.05$, $P < 0.01$, and $P < 0.001$ were considered statistically significant. NS, not significant.

wound inspection at the histological level, leading to a group size of $n = 3$ for day 5 (data not shown). Histological evaluation of wounds confirmed that the IEC layer in *Chop*$^{\text{IEC Tg/Tg}}$ mice was not completely reconstituted even 5 days after wound induction, whereby no signs of apoptosis were found in the wound regions (**Figure 6c**). Immunofluorecence staining for Vimentin and CD19 indicated a more profound fibrosis with concurrently reduced infiltration of B cells in the wound beds of transgenic mice. (**Figure 6d,e**). This is in line with literature indicating CD19-positive B cells to actively promote cutaneous wound healing.[30] An enhanced presence of CD19-positive B cells in the mucosa was also confirmed during recovery from DSS treatment (but not after 3 days of DSS treatment), with no significant differences between transgenic and WT mice (**Figure 6f,g**). Using the mechanical injury approach, we were able to show that *Chop*$^{\text{IEC Tg/Tg}}$ mice are impaired in their wound-healing capacity, independently of different grades of inflammation similar to that in the DSS experiments.

IEC-specific overexpression of CHOP protein affects cell proliferation

A possible explanation for the phenotype observed in the mucosal wound-healing assay would be an altered IEC proliferation behavior. Even though CHOP is widely discussed as an apoptosis-related protein, recently published studies suggest a functional correlation between CHOP expression and proliferation.[16,31–33] Yet, in untreated *Chop*$^{\text{IEC Tg/Tg}}$ mice, the numbers of Ki-67-positive IECs remained unaltered, indicating no changes in the total number of cells in active phases of the cell cycle (G1, S, G2, and mitosis) (**Figure 3d**). To further investigate whether CHOP causes functional disturbances in IEC proliferation, *in vivo* bromodeoxyuridine (BrdU) labeling was performed in untreated mice. BrdU is only incorporated into newly synthesized DNA during the S phase of the cell cycle, therefore giving a picture distinct from Ki-67 (**Figure 7a**). Indeed, while the numbers of colonic Ki-67-positive cells remained unaltered, the numbers of BrdU-positive cells were

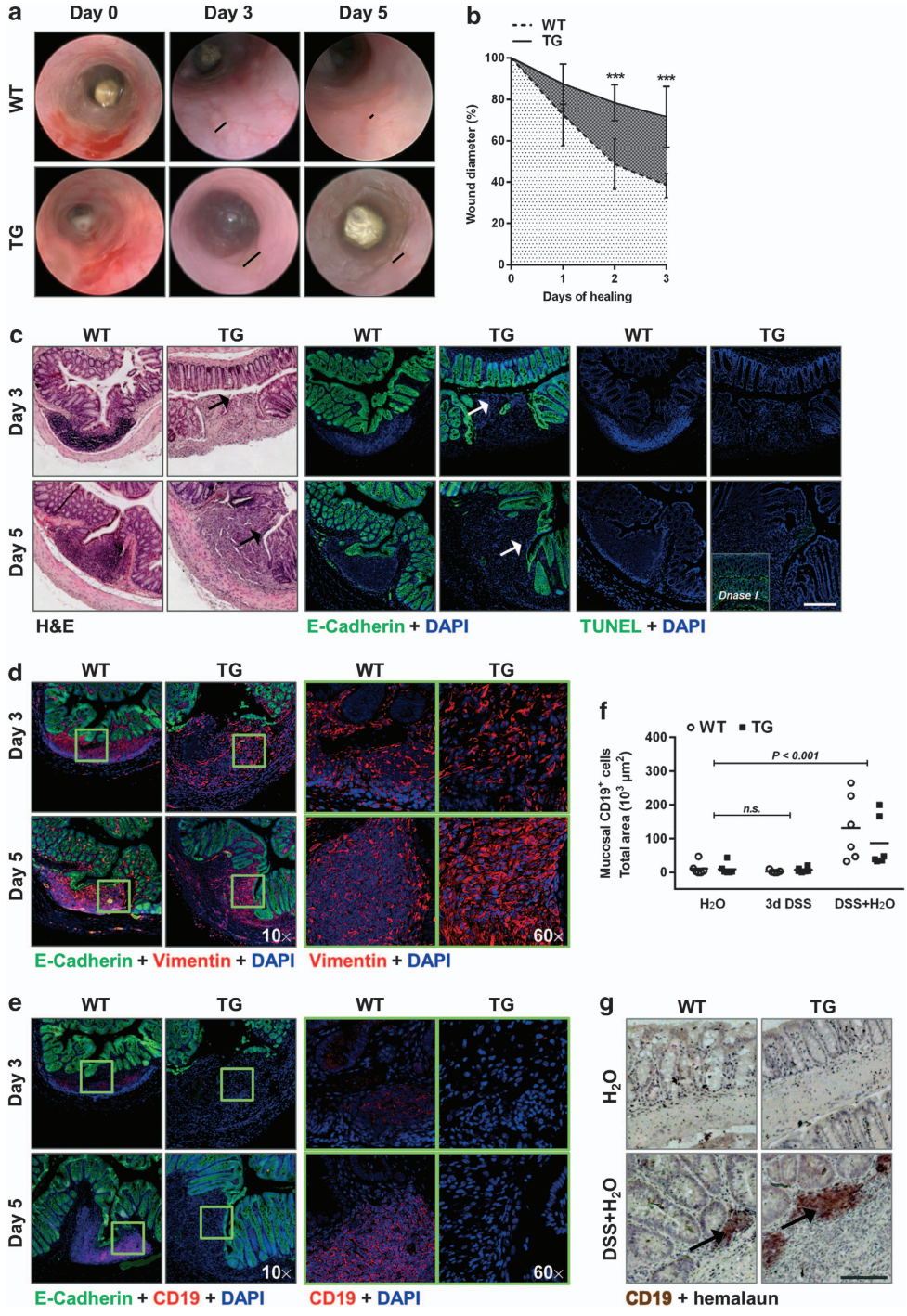

Figure 6 Wound healing is impaired in *Chop*$^{IEC\ Tg/Tg}$ mice. (**a**) Colonic mucosal lesions were mechanically induced in *Chop*$^{IEC\ Tg/Tg}$ mice and wild-type (WT) controls using a biopsy clamp. Wound healing was monitored by video colonoscopy on days 0, 1, 2, 3, and 5. (**b**) Wound diameters were calculated as percentage to initial wound size. Statistical significance was assessed by non-parametric rank-sum test, $^{*}P<0.05$,$^{**}P<0.01$, and $^{***}P<0.001$ were considered statistically significant. (**c**) Wound sections of *Chop*$^{IEC\ Tg/Tg}$ mice and WT controls were stained with hematoxylin and eosin (H&E). Immunofluorescence staining was performed by using anti-E-Cadherin antibody as intestinal epithelial cell marker protein. Terminal deoxinucleotidyl transferase-mediated dUTP-fluorescein nick end labeling (TUNEL) assay was performed on wound sections of transgenic (TG) mice and WT controls. Positive controls were treated with DNaseI. (**d**, **e**) Immunofluorescence staining of wound sections using E-Cadherin and Vimentin (**d**) and E-Cadherin and CD3 (**e**) antibodies. 4,6-Diamidino-2-phenylindole (DAPI) was used for nuclear counterstain. Bar = 200 µm. Disintegrated epithelial layer is indicated by arrows. (**f**) The numbers of infiltrating CD19+ cells were determined by applying the respective antibody on tissue sections of distal colon (dC) from TG mice and WT controls ($n = 5$–6). Data sets of water-treated as well as 3d and 5d dextran sodium sulfate (DSS)-treated + 5d recovery period TG and WT mice were analyzed by two-way ANOVA with genotype and DSS treatment as main factors followed by multiple comparison procedure by Holm–Sidak method, $P<0.001$ was considered statistically significant. (**g**) Representative pictures of dC tissue sections from water-treated and 5d DSS-treated + 5d recovery period TG and WT control stained for CD19. Bar = 100 µm. NS, not significant.

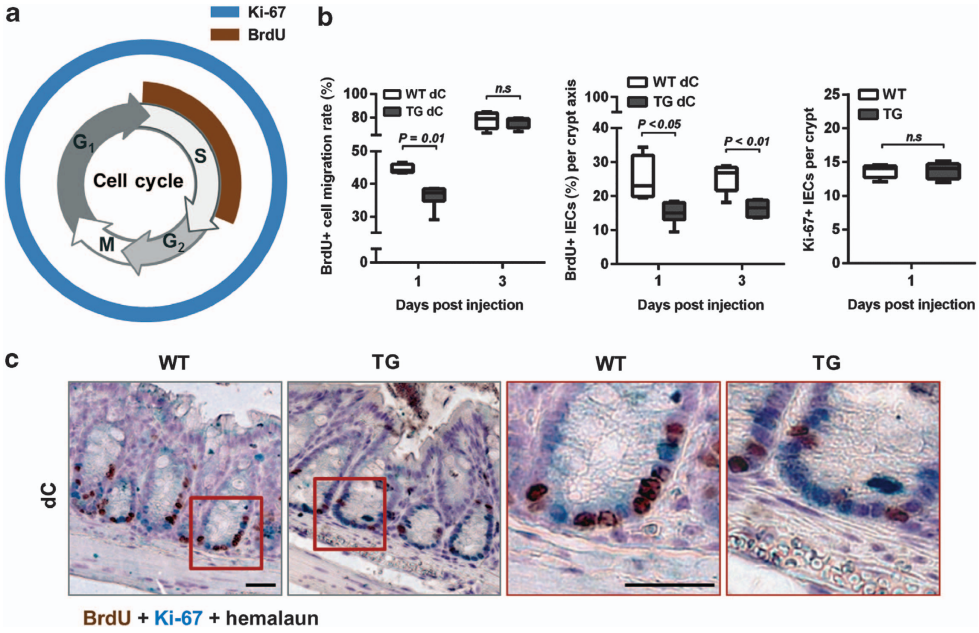

Figure 7 *Chop*$^{IEC\ Tg/Tg}$ mice exhibit changes in cell cycle progression. (**a**) Schematic illustration of the stages of cell cycle with possible detection of proliferation markers Ki-67 and bromodeoxyuridine (BrdU), respectively. (**b**) Cell cycle progression was analyzed by BrdU labeling of transgenic (TG) mice and wild-type (WT) controls ($n=5$). Detection of BrdU-positive and Ki-67-positive cells, respectively, was performed by immunohistochemistry on tissue sections of distal colon (dC). The migration rate was calculated as the percentage of the distance reached by BrdU-positive cells relative to the crypt depth. The numbers of BrdU-positive cells are given as the percentage of total colonic epithelial cells per crypt axis. The numbers of Ki-67-positive cells were counted per crypt. All data sets are presented as means ± s.d. Statistical significance was assessed by non-parametric rank-sum, $P<0.05$, $P<0.01$, and $P<0.001$ were considered statistically significant. (**c**) Representative colonic tissue sections from TG mice and WT controls illustrate reduced numbers of BrdU-positive epithelial cells (brown) in *Chop*$^{IEC\ Tg/Tg}$ mice, while total numbers of Ki-67-positive intestinal epithelial cells (IECs; blue) remained unaffected. Bars = 50 μm. NS, not significant.

reduced concomitantly with a slower migration rate of IEC (**Figure 7b,c**).

Transgenic CHOP is posttranscriptionally modified and affects cell cycle progression *in vitro*

As the results from the BrdU labeling suggested impaired IEC proliferation, we addressed the question of the mechanistic role of CHOP in cell cycle progression *in vitro*. Comparing protein isolates from the colonic IEC line ptk6 transiently transfected with CHOP-HA and colonic IEC isolates from *Chop*$^{IEC\ Tg/Tg}$ mice, both exhibited a similar banding pattern for CHOP-HA protein (**Figure 8a**). Again, a slight shift in molecular weight was observed, indicative of posttranslational modifications. In line, Wang and Ron[19] found CHOP to be phosphorylated by the p38 mitogen-activated protein (MAP) kinase at serine residues 78 and 81, which seemed to be crucial for the transcriptional activation of CHOP. Even though we demonstrated CHOP-HA to be nuclear localized in *Chop*$^{IEC\ Tg/Tg}$ mice (**Figure 2d**), we choose to generate a mutant form of CHOP with the specific serine residues replaced by alanine [S78/81A], enabling us to investigate the impact of phosphorylated and non-phosphorylated CHOP on cell cycle progression. Analysis of stably transfected ptk6:CHOP-HA and ptk6:[S78/81A] cells demonstrated CHOP-HA protein to be posttranslationally modified at the p38 MAP kinase-specific phosphorylation sites (**Figure 8b**). Interestingly, both CHOP-HA as well as CHOP-HA[S78/81A] were found to be nuclear localized, indicating CHOP to act as transcription factor independently of the phosphorylation status of the serine residues 78 and 81 (**Figure 8c**). Overexpression of both proteins lead to decreased ptk6 cell proliferation, which was not associated with enhanced apoptosis or necrosis (**Figure 8d,e**). As Barone *et al.* reported that CHOP might impact on cell cycle progression by inducing an G1 arrest,[34] we used propidium iodide DNA staining and flow cytometry to assess the impact of CHOP-HA and CHOP-HA[S78/81A] on epithelial cell cycle. Indeed, CHOP-HA caused an accumulation of cells in G1 concomitant with the decreased numbers of cells in G2, yet, overexpression of CHOP-HA[S78/81A] resulted in the increased numbers of cells in G2 and reduced the numbers of cells in the G1 phase (**Figure 8f,g**). These results were reflected in an *in vitro* scratch closure assay, which showed a delayed wound closure for cells overexpressing both forms of CHOP (see **Supplementary Figure S4**). The effect was even more pronounced in ptk6:[S78/81A] cells.

DISCUSSION

The activation of UPR signaling in the epithelium of IBD patients and the data on the concurrent downregulation of the UPR target gene CHOP appear to be in conflict.[28] We confirmed these findings in three independent mouse models, T-cell-mediated and bacteria-driven chronic colitis as well as

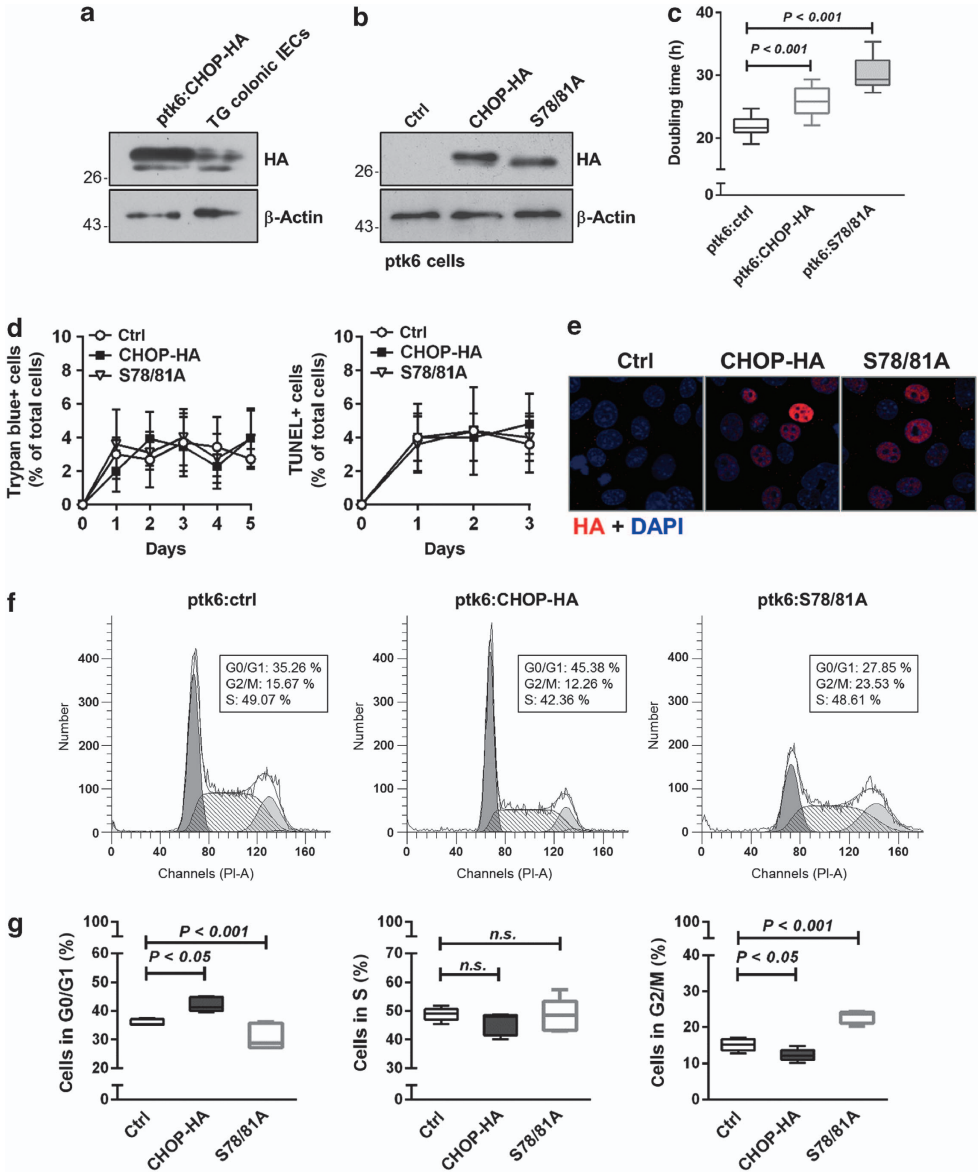

Figure 8 *In vitro* data indicate C/EBP homologous protein (CHOP)-mediated accumulation of epithelial cells in G1 and G2. (**a**) Analysis of transgenic (TG) CHOP expression in the transfected colonic epithelial ptk6 cell line and colonic intestinal epithelial cell isolates from *Chop*$^{IEC\ Tg/Tg}$ mice was performed by western blotting using anti-HA antibody. Anti-β-actin was used a as loading control. (**b**) Generation of CHOP-HA mutant [S78/81A]. The p38 mitogen-activated protein kinase-specific phosphorylation sites, serine-residues 78 and 81, have been replaced by alanine. Transgene expression was detected by western blotting using anti-HA antibody on cell lysates of CHOP-HA, CHOP-HA [S78/81A], and (**c**) doubling time of stable cell lines ptk6:ctrl, ptk6:CHOP-HA, and ptk6:[S78/81A] was assessed using BrdU (bromodeoxyuridine) proliferation assay. Data are presented as means ± s.d. Non-parametric rank-sum test was performed. $P<0.05$, $P<0.01$, and $P<0.001$ were considered statistically significant. (**d**) Markers of cell death were monitored in stable cell lines ptk6:ctrl, ptk6:CHOP-HA, and ptk6:[S78/81A]. Twenty thousand cells per ml were seeded into 24-well plates, and the numbers of necrotic cells were analyzed by trypan blue staining for 5 days ($n=8$). Also, 100,000 cells ml^{-1} seeded into 24-well plates, and the numbers of apoptotic cells were assessed by terminal deoxinucleotidyl transferase-mediated dUTP-fluorescein nick end labeling (TUNEL) assay ($n=4$). The numbers of necrotic and apoptotic cells were calculated as the percentage of total cells. All data are plotted as mean ± s.d. (**e**) Immunofluorescence staining was performed on stable cell lines ptk6:ctrl, ptk6:CHOP-HA, and ptk6:[S78/81A] by applying anti-HA antibody. 4,6-Diamidino-2-phenylindole (DAPI) was used for nuclear counterstain. (**f**) Cell cycle progression of stable cell lines ptk6:ctrl, ptk6:CHOP-HA, and ptk6:[S78/81A] cells was determined by fluorescence-activated cell sorting (FACS) analysis by performing propidium iodide staining ($n=5$). (**g**) FACS data are presented as means ± s.d. Statistical significance was assessed by non-parametric rank-sum test. $P<0.05$, $P<0.01$, and $P<0.001$ were considered statistically significant. NS, not significant.

DSS-induced acute colitis; however, the mechanism of CHOP downregulation remains elusive.

Most insights into the functional role of CHOP in the context of intestinal inflammation have been gained in studies using complete CHOP knockout mice. These mice show a decreased susceptibility towards DSS and 2,4,6-trinitrobenzenesulfonic acid challenges. This effect was attributed to reduced pro-apoptotic signaling in the mucosa likely as a consequence of

lower numbers of infiltrating macrophages and subsequently reduced oxidative stress levels.[27,35] To further investigate the functional role of CHOP downregulation under inflammatory conditions in IECs, we generated a novel IEC-specific mouse model transgenic for CHOP.

In line with the data from the CHOP knockout mice, *Chop*$^{IEC\ Tg/Tg}$ mice were more susceptible to DSS-induced colitis and show increased numbers of infiltrating macrophages and antigen-presenting cells at the early time point. Yet, *Chop*$^{IEC\ Tg/Tg}$ mice did neither show a spontaneous phenotype nor substantially increased IEC apoptosis even after acute 3d DSS challenge. As *Chop*$^{IEC\ Tg/Tg}$ mice show more pronounced mucosal damage, the slight increase of cC3-positive IECs seen in response to 3d DSS treatment might simply reflect a more severe disease stage. Particularly, when considering that the overall difference between WT and *Chop*$^{IEC\ Tg/Tg}$ mice was minor compared with the induction of apoptosis in the DSS-treated vs. control groups. The same holds true for the pro-apoptotic CHOP target genes *Gadd34* and *Ero1α*. Both exhibited only a minor elevation of expression in *Chop*$^{IEC\ Tg/Tg}$ mice compared with wild-type animals after 3d DSS challenge. In addition, these genes seemed to be regulated independently of CHOP[36] in this setup, as wild-type animals show induced expression levels despite the fact of lowered CHOP protein expression. In CHOP knockout mice, the decreased susceptibility to chemically induced colitis has been attributed, at least in part, to reduced expression levels and subsequently decreased *Ero1α*-mediated reactive oxygen species production.[27]

Taking on the sporadic reports from literature stating a role for CHOP in proliferation[16,31–33] and cell cycle progression,[34] we found compelling evidence for CHOP-mediated retardation of IEC proliferation. The patchy distribution of lesions induced by DSS made it impossible to evaluate whether recovery of mice was delayed owing to impaired re-epithelialization and IEC proliferation or enlarged wounds. However, investigating mechanically induced colonic injuries confirmed transgenic mice to be retarded in mucosal healing independent of acute inflammation or enhanced apoptosis. Decreased tissue regeneration in *Chop*$^{IEC\ Tg/Tg}$ mice was associated with lower numbers of mucosal-infiltrating CD19-positive lymphocytes, which have recently been reported to contribute to wound healing in skin tissue.[30] In contrast, during recovery from DSS treatment, WT and transgenic mice displayed equal numbers of CD19-positive cells in the mucosa, suggesting that infiltration of cells was just delayed, but not diminished in mechanically *Chop*$^{IEC\ Tg/Tg}$ mice.

Intestinal wound healing comprises three cellular events with regard to re-epithelialization, IEC restitution, proliferation and differentiation.[37] In the context of DSS, Araki *et al.*[38] demonstrated that the onset of colitis was promoted by reduced epithelial turnover rates associated with enhanced apoptosis of IEC. BrdU labeling of disease-free *Chop*$^{IEC\ Tg/Tg}$ mice revealed reduced numbers of BrdU-positive IECs with concurrently retarded IEC migration rates. As the total numbers of proliferative colonic IECs remained unaffected, we assume that the numbers of cells entering the S phase for DNA replication is reduced, which in turn results in an accumulation of IEC in G1. These findings, which were also confirmed *in vitro*, are appealing for explaining the phenotype observed in the challenged *Chop*$^{IEC\ Tg/Tg}$ mice. In conclusion, the downregulation of CHOP might represent a protective mechanism promoting IEC proliferation to enhance mucosal healing in response to inflammatory or exogenous injuries (**Figure 9**). Our data furthermore suggest that the regulation of CHOP was independent of activated UPR signaling in mouse models of acute and chronic colitis and that IEC-specific overexpression of CHOP impaired epithelial integrity independently of apoptotic mechanisms. Consistently, recent studies demonstrate that mice carrying epithelial cell–specific modifications in genes implicated in cell proliferation and survival display delayed epithelial regeneration in response to acetic acid–induced ulceration, mechanical injury, and DSS treatment.[39–41]

Although CHOP-induced defects in IEC proliferation might diminish the regenerative ability of the epithelial lining, epithelial integrity was maintained under non-challenged conditions. Noteworthy, CHOP can be posttranslationally modified by various kinases and does not possess a functional nuclear localization site, making nuclear translocation strongly dependent on heterodimer formation.[16,19] In this context, phosphorylation at serine residues 79/82 (human) and 78/81 (mouse) by the stress-induced p38 MAP kinase has been associated with enhanced transcriptional activity of CHOP following prolonged ER stress, favoring apoptosis of affected cells.[19] Our *in vitro* data suggest CHOP-HA to be partly modified by phosphorylation at the p38 MAP kinase-specific phosphorylation sites, resulting in a band pattern also observed in *Chop*$^{IEC\ Tg/Tg}$ mice. However, we could not find evidence for altered phosphorylation patterns in response to mucosal insults *in vivo*, and also the *in vitro* data indicated that effects of CHOP on IEC proliferation were independent of its phosphorylation status at serine residues 78/81. Yet, CHOP-HA caused accumulation of cells in G1 while the mutant form resulted in G2 accumulation, pointing to the possibility that even though the impact on cell cycle seems to be specific, it might be mediated by different binding partners of phosphorylated and unphosphorylated CHOP. Under non-diseased conditions, *Chop*$^{IEC\ Tg/Tg}$ mice seemed to be able to compensate for, or to be unaffected by, the slower migration rate of IECs. This is true despite the fact that CHOP is implicated in Wnt-signaling pathways[42] as well as in mechanisms underlying the loss of stem cell properties.[31] This might be due to the Villin-driven Cre expression, which might preferentially target transit-amplifying cells rather than Lgr5-positive stem cells, causing reduced proliferation rates predominantly in transit-amplifying cells.

Increasing rates of both IEC proliferation and apoptosis have been observed in UC patients, while CHOP mRNA and protein expression were shown to be reduced in UC.[28,43,44] According to our data, high CHOP expression in IEC could promote disease progression in IBD, while the downregulation of CHOP in UC might reflect a protective mechanism underlying the regulation of IEC proliferation in inflamed tissue. Notably,

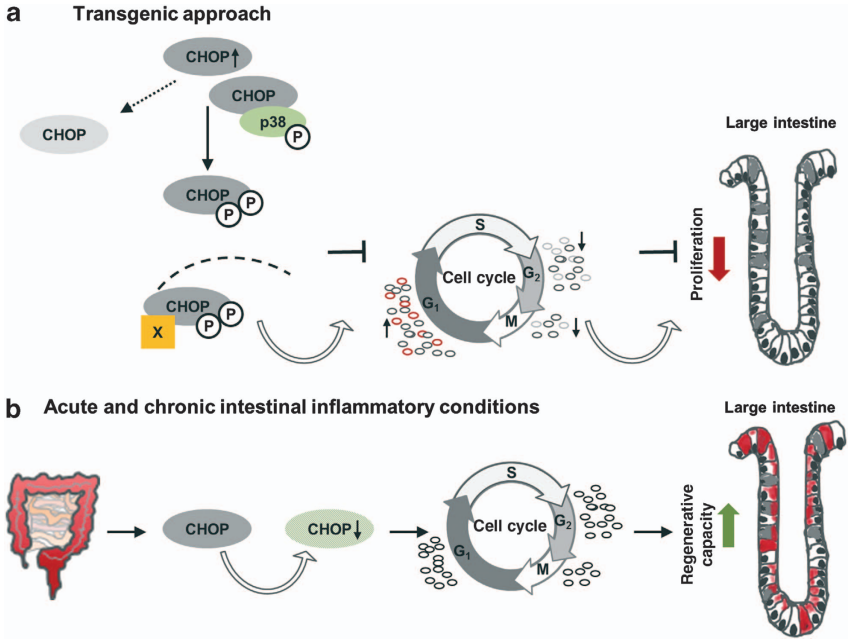

Figure 9 Postulated mechanism of C/EBP homologous protein (CHOP) downregulation under acute and chronic inflammatory conditions. (**a**) Summarized results of the transgenic approach using *Chop*$^{IEC\ Tg/Tg}$ mice. Overexpression of CHOP protein results in increased posttranslational modification of CHOP at p38-specific phosphorylation sites, serine residues 78 and 81. As CHOP is suggested to lack a functional nuclear localization signal, nuclear translocation is mediated by heterodimer formation with CHOP-binding partner X. Enhanced CHOP protein expression impacts on cell cycle progression by inducing accumulation of cells in G1, which *in vitro* is rather associated with depletion of cells in G2/M. The CHOP-mediated delay in cell cycle progression is suggested to lead to the impaired proliferative capacity of colonic intestinal epithelial cell in transgenic mice, which consequently affects the cell migration rate along the crypt axis associated with impaired epithelial cell regeneration upon colonic mucosal injury. (**b**) Proposed function of CHOP downregulation in response to acute and chronic intestinal inflammatory conditions. Downregulation of CHOP at the level of mRNA and protein expression is suggested to contribute to protective mechanisms involved in the maintenance of epithelial cell proliferation upon inflammatory conditions.

persistent IBD is associated with steadily rising risk for developing colorectal cancer.[45] These findings suggest that clinical therapies in acute disease need to maintain low expression levels of CHOP to promote a fast healing process in the colon, while patients in remission may require higher CHOP level to inhibit uncontrolled proliferation and tumor development.

METHODS

All animal procedures were approved by the Institutional Animal Care and Use Committee, University of North Carolina at Chapel Hill, NC or approved by the Bavarian Animal Care and Use Committee (AZ 55.2-1-54-2531-164-09, AZ 55.2-1-54-2532-160-12, AZ 55.2-1-54-2532-165-12).

Adoptive T-cell transfer and bacterial associations. Adoptive T -cell transfer experiments and bacterial mono- and dual-association with colitogenic *E. faecalis* and/or *E. coli* were performed as previously described.[8] IECs were isolated from cecal and colonic tissues and pooled for mRNA and protein expression analysis, respectively. Histological scores were blindly assessed for cecal and colonic tissues, and means were calculated.

Generation of *Chop*$^{Rosa26\ flox/flox}$ WT controls. C57BL/6N mice were used for knock-in mutagenesis to generate the *Chop*$^{Rosa26\ flox/flox}$ strain purchased from Taconic (TaconicArtemis GmbH, Cologne, Germany). Therefore, a construct containing the high responsive CAGGS promoter and coding sequence for murine CHOP protein with HA tagged to the C-terminus was introduced into the Rosa26 locus. Promoter-associated floxed STOP sequence inhibits the expression of the transgene.

Generation of homozygote *Chop*$^{IEC\ Tg/Tg}$ mouse model. Homozygote *Chop*$^{Rosa26\ flox/flox}$ females were mated with males expressing Cre recombinase under the control of a 9-kb regulatory region of mouse villin promoter.[46] Homozygote *Chop*$^{Rosa26\ flox/flox}$ and *Chop*$^{IEC\ Tg/Tg}$ mice were used for intercrossed breeding to generate adequate WT controls and conditionally CHOP-HA overexpressing mice (TG).

Chromoendoscopy. Chromoendoscopy was performed using 1% methylene blue (Sigma-Aldrich, Taufkirchen, Germany). Colonic crypt pattern were analyzed by video colonoscopy (KARL STORZ GmbH, Tuttlingen, Germany).

DSS-induced colitis. Male littermates aged 12 weeks received 2% (w/v) DSS (MP Biomedicals, Eschwege, Germany) in drinking water for 3 and 7 days. Examination of epithelial repair in experimental colitis was performed by providing 2% (w/v) DSS in drinking water for 5 days followed by a period of 5 days for recovery. Disease Activity Index was scored daily as previously described.[8] After treatment, mice were killed by CO_2. The colon was opened longitudinally and carefully cut into two pieces. One half was used for IEC isolation, the other one was fixed in 4% neutral-buffered formalin.

Histopathological analysis. Histological scoring was performed on hematoxylin and eosin–stained tissue sections by blindly assessing the degree of inflammation as previously described.[47] Colonic tissue sections were scored for epithelial damage (0 = normal; 1 = hyperproliferation, irregular crypts, and goblet cell loss; 2 = mild-to-moderate crypt loss (10–50%); 3 = severe crypt loss (50–90%); 4 = complete crypt loss, surface epithelium intact; 5 = small-to medium-sized ulcer (<10 crypt widths); and 6 = large ulcer (⩾10 crypt

widths)) and infiltration of inflammatory cells (mucosa (0 = normal, 1 = mild, 2 = modest, 3 = severe), submucosa (0 = normal, 1 = mild to modest, 2 = severe), and muscle/serosa (0 = normal, 1 = moderate to severe)). Calculated mean scores ranged from 0 (not inflamed) to 12 (massively inflamed). For mono- and dual-association experiments, histopathological scores were assigned as previously described.[48]

***In vivo* wound-healing assay**. *In vivo* wound healing was performed as previously described.[49] Mice were anesthetized using isoflurane inhalational anesthesia. Colonic mucosal lesions with a diameter of 800 μm were induced in $Chop^{Rosa26\ flox/flox}$ and $Chop^{IEC\ Tg/Tg}$ mice ($n = 6$) using a biopsy clamp. Wound healing was monitored by video colonoscopy (KARL STORZ GmbH) on days 0, 1, 2, 3, and 5 and assessed by calculating wound diameter relative to initial wound size. Mice were killed by cervical dislocation on days 3 and 5 ($n = 3$ per group and day), and colonic tissue, including the wound region, was fixed in 4% neutral-buffered formalin.

***In vivo* BrdU labeling**. $Chop^{IEC\ Tg/Tg}$ mice and WT controls were intraperitoneally injected with BrdU labeling reagent (Life Technologies GmbH, Karlsruhe, Germany). Mice ($n = 5$) were killed on days 1 and 3 after injection by cervical dislocation. Colonic tissue was fixed in 4% neutral-buffered formalin for paraffin embedding. Detection of BrdU-positive cells was performed by using the BrdU In-situ Detection Kit following the manufacturer's instructions (BD Biosciences, Heidelberg, Germany).

Laser capture microdissection. A total area of 2,000,000 μm^2 was microdissected from epithelium, lamina propria, and muscularis by using the UV laser-cutting system LMD 6000 and the Leica Application Suite software (Leica Microsystems GmbH, Nussloch, Germany). Total RNA was prepared using RNeasy Micro Kit (Qiagen, Hilden, Germany) according to the manufacturer's instructions.

Isolation of IECs. IECs were isolated by subsequent incubation of the intestine in Dulbecco's modified Eagle's medium and phosphate-buffered saline (PBS) supplemented with 10 mM dithiothreitol and 1.5 mM EDTA, respectively, as further described in **Supplementary Methods**.

Histology and tissue staining. Intestinal tissue fixed in 4% neutral-buffered formalin was used for paraffin embedding (Leica Microsystems GmbH). Tissue staining, immunohistochemistry, and immunofluorescence were performed as described in **Supplementary Methods**.

Gene expression analysis. Total RNA was isolated using the column-based NucleoSpin RNAII kit (*Macherey*-Nagel GmbHDüren, Germany) according to the manufacturer's instructions. Complementary DNA was prepared using the SuperScript First-Strand Synthesis System (Life Technologies GmbH). Quantification of gene expression was performed on LightCycler 480 System using the Universal ProbeLibrary System (Roche Diagnostics GmbH, Mannheim, Germany) and gene-specific primers for CHOP *for_5′-AGCTAGCTG TGCCACTTTCC-3′, rev_5′-GGGAAGCAACGCATGAAG-3′;* Ero1α *for_5′-TCGAAGTGCAAAGGAAATGA-3′*, *rev_5′-GCGTCCAGATTT TCAGCTCT-3′*; and Gadd34 *for_5′-AGCTGAATCCAAATCGCTGT-3′*, *rev_5′-TCTGTACTGGAAATGCCTTCCT-3′* (Sigma-Aldrich).

Western blotting analysis. Total protein concentration of ultrasonicated samples was determined by Bradford Assay (Carl Roth GmbH, Karlsruhe, Germany) according to the manufacturer's instructions. Sample volumes containing 20 μg of protein were diluted with 5 × sodium dodecyl sulfate buffer and incubated for 10 min at 95 °C. Also, 12.5% reducing sodium dodecyl sulfate polyacrylamide gel electrophoresis was performed followed by semi-dry blotting using polyvinylidene difluoride membranes. Blocking was performed using 5% milk powder/1 × TBS/0.1% Tween-20 (TBST) for 1 h at room temperature (RT). Primary antibodies anti-HA (1:1000, 14-6756, eBioscience, Frannkfurt, Germany), anti-CHOP (1:1000, sc-575, Santa Cruz Biotechnology, Heidelberg, Germany), anti-GRP78 (1:4000, G9043, Sigma-Aldrich), and anti-β-actin (1:2000, no.4970, Cell Signaling Technology, Frankfurt, Germany; 1:1000, ICN, Costa Mesa, CA) were applied overnight at 4 °C. Membranes were washed three times with TBST. Incubation with appropriate horseradish peroxidase–conjugated secondary antibody anti-rabbit (1:4000, Dianova, Hamburg, Germany) was carried out for 1 h at RT followed by washing with TBST. The respective immunoreactive protein was detected by using an enhanced chemiluminescence light-detecting kit (GE Healthcare, Uppsala, Sweden).

Generation of pcDNA3.1(-)-CHOP-HA. Total RNA was extracted from C57BL/6N embryo 7.5 dpc (*Macherey*-Nagel GmbH), and cDNA library was generated by using the SuperScript Reverse Transcriptase (Life Technologies GmbH). Cloning of Gadd153 cDNA was performed by using primer pairs *for_5′-TATCATGTTGAAGATGAGCGGGTG-3′*, *rev_5′-caatgtaccgtctatgtgcaagcc-3′*, and *for_5′-AGAATTCACCATGG CAGCTGAGTCCCTGC-3′*, *rev_5′-AGCGGCCGCTGCTTGGTGCA GG-3′* (Sigma-Aldrich). PCR product and HA-tag oligomer were digested with NotI and ligated using the Quick Ligation Kit following the manufacturer's instructions (New England Biolabs, Frankfurt, Germany). Ligation product was amplified by using primer pairs *for_5′-AGAATTCACCATGGCAGCTGAGTCCCTGC-3′* and *rev_5′-A GGATCCCTAAGCGTAATCTGGAACATCGTATGGG-3′* and inserted into pcDNA3.1(-)-Hygro by using EcoRI and BamHI restriction sites (New England Biolabs).

Site-directed mutagenesis. Site-directed mutagenesis of CHOP-HA was performed by overlap extension PCR using Phusion Hot Start II High-Fidelity DNA Polymerase (New England Biolabs). Following primer pairs were used to create CHOP-HA mutant [S78/81A]: S78/81A *for_5′-ACACGCACATCCCAAGCCCCTCGCGCTCCAGAT TCCAGTCAGAG-3′* and *rev_5′-CTCTGACTGGAATCTGGAGCGCG AGGGGCTTGGGATGTGCGTGT-3′*. PCR reactions were performed using the cycle conditions: 1 × 3 min at 95 °C; 25 × 1 min at 95 °C, 1 min at 52 °C, 1 min at 72 °C; and 1 × 7 min at 72 °C.

Cell culture and transfection. Ptk6 cells were cultured in RPMI1640 as previously described.[50] Plasmid DNA transfection was performed by using Fugene 6 (Promega, Mannheim, Germany).

Determination of cellular proliferation, necrosis, and apoptosis. Determination of ptk6 cell proliferation was performed by using Cell Proliferation enzyme-linked immunosorbent assay and BrdU labeling following the manufacturer's instructions (Roche Diagnostics). Markers of cell death were monitored in stable ptk6 cell lines by seeding 20,000 cells ml^{-1} into 24-well plates and determining the numbers of necrotic cells by trypan blue staining. For TUNEL (terminal deoxinucleotidyl transferase-mediated dUTP-fluorescein nick end labeling) assay, 100,000 cells ml^{-1} were seeded into 24-well plates and the numbers of apoptotic cells were assessed by using the ApoBrdU DNA Fragmentation Assay Kit according to the manufacturer's instructions (K401-60, BioVision, Heidelberg, Germany).

Flow cytometry. Polyclonal cell lines ptk6:ctrl, ptk6:CHOP-HA, and ptk6:CHOP-HA [S78/81A] (2×10^4 cells ml^{-1}) were seeded into T-25 cell culture flasks ($n = 5$) (Sarstedt AG, Nümbrecht, Germany) and cultivated in media supplemented with interferon-γ at 33 °C. When cell monolayers reached 70% confluency, cells were detached using Trypsin/EDTA (Life Technologies GmbH) and resuspended by pipetting to single cells. Five milliliters of medium was added, and cells were centrifuged at 300 *g* for 5 min. Cell pellets were resuspended in 5 ml ice-cold PBS (Life Technologies GmbH) and centrifuged at 300 *g* for 5 min. For fixation, cells were incubated in 2 ml ice-cold 70% ethanol on ice for 1 h. Later, cells were centrifuged at 300 *g* for 5 min and washed twice with 1 ml ice-cold PBS. A total of 100 μl RNase-solution (100 μg ml^{-1} in PBS) was added, and cells were incubated for 5 min at RT. Also, 800 μl propidium iodide solution (50 μg ml^{-1} in PBS) was added, and cells were incubated for additional 15 min at RT

and 10 min at 37 °C. A total of 20,000 cells were analyzed using the BD FACSDiva software (BD Biosciences).

Statistical analysis. All statistical computations were performed by using SigmaPlot 11.0 (Systat software, Erkrath, Germany). Differences between groups were considered statistically significant if $P < 0.05$.

SUPPLEMENTARY MATERIAL is linked to the online version of the paper at http://www.nature.com/mi

ACKNOWLEDGMENTS

We thank Michael Allgäuer for help with the *in vivo* BrdU labeling; Sebastian Wolfshöfer and Tiago Nunes supported our work by help with the *in vivo* wound-healing assay. This work was supported by Die Deutsche Forschungsgemeinschaft grant GE 2042/2-1 to M.G.

AUTHOR CONTRIBUTIONS

N.W., E.B., .E.R., and D.H. conceived and designed the experiments. E.B. generated the HA-tagged CHOP construct for the mouse model *Chop*$^{Rosa26\ flox/flox}$. N.W. did most of the experiments and data analysis. N.W., E.R., and D.H. wrote the paper. M.H. contributed to immune cell staining. M.G. highly contributed to the BrdU labeling. B.W. highly contributed to the *in vivo* wound-healing assay. K.P.J. kindly provided *vil-Cre* mice. B.W. and D.H. contributed reagents, material, and analysis tools.

DISCLOSURE

The authors declared no conflict of interest.

REFERENCES

1. McGovern, D.P. *et al.* Genome-wide association identifies multiple ulcerative colitis susceptibility loci. *Nat. Genet.* **42**, 332–337 (2010).
2. Imielinski, M. *et al.* Common variants at five new loci associated with early-onset inflammatory bowel disease. *Nat. Genet.* **41**, 1335–1340 (2009).
3. Maeda, S. *et al.* Nod2 mutation in Crohn's disease potentiates NF-kappaB activity and IL-1beta processing. *Science* **307**, 734–738 (2005).
4. Kontoyiannis, D. *et al.* Genetic dissection of the cellular pathways and signaling mechanisms in modeled tumor necrosis factor-induced Crohn's-like inflammatory bowel disease. *J. Exp. Med.* **196**, 1563–1574 (2002).
5. Muise, A.M. *et al.* Polymorphisms in E-cadherin (CDH1) result in a mis-localised cytoplasmic protein that is associated with Crohn's disease. *Gut* **58**, 1121–1127 (2009).
6. Consortium, U.I.G. & Barrett, J.C. *et al.* Genome-wide association study of ulcerative colitis identifies three new susceptibility loci, including the HNF4A region. *Nat. Genet.* **41**, 1330–1334 (2009).
7. Kaser, A. *et al.* XBP1 links ER stress to intestinal inflammation and confers genetic risk for human inflammatory bowel disease. *Cell* **134**, 743–756 (2008).
8. Rath, E. *et al.* Induction of dsRNA-activated protein kinase links mitochondrial unfolded protein response to the pathogenesis of intestinal inflammation. *Gut* **61**, 1269–1278 (2012).
9. Tabas, I. & Ron, D. Integrating the mechanisms of apoptosis induced by endoplasmic reticulum stress. *Nat. Cell Biol.* **13**, 184–190 (2011).
10. Ron, D. & Habener, J.F. CHOP, a novel developmentally regulated nuclear protein that dimerizes with transcription factors C/EBP and LAP and functions as a dominant-negative inhibitor of gene transcription. *Genes Dev.* **6**, 439–453 (1992).
11. Oyadomari, S. & Mori, M. Roles of CHOP/GADD153 in endoplasmic reticulum stress. *Cell Death Differ.* **11**, 381–389 (2004).
12. Hattori, T., Ohoka, N., Inoue, Y., Hayashi, H. & Onozaki, K. C/EBP family transcription factors are degraded by the proteasome but stabilized by forming dimer. *Oncogene* **22**, 1273–1280 (2003).
13. Ubeda, M., Schmitt-Ney, M., Ferrer, J. & Habener, J.F. CHOP/GADD153 and methionyl-tRNA synthetase (MetRS) genes overlap in a conserved region that controls mRNA stability. *Biochem. Biophys. Res. Commun.* **262**, 31–38 (1999).
14. Jousse, C. *et al.* Inhibition of CHOP translation by a peptide encoded by an open reading frame localized in the chop 5'UTR. *Nucleic Acids Res.* **29**, 4341–4351 (2001).
15. Ohoka, N., Hattori, T., Kitagawa, M., Onozaki, K. & Hayashi, H. Critical and functional regulation of CHOP (C/EBP homologous protein) through the N-terminal portion. *J. Biol. Chem.* **282**, 35687–35694 (2007).
16. Chiribau, C.B., Gaccioli, F., Huang, C.C., Yuan, C.L. & Hatzoglou, M. Molecular symbiosis of CHOP and C/EBP beta isoform LIP contributes to endoplasmic reticulum stress-induced apoptosis. *Mol. Cell. Biol.* **30**, 3722–3731 (2010).
17. Chen, B.P., Wolfgang, C.D. & Hai, T. Analysis of ATF3, a transcription factor induced by physiological stresses and modulated by gadd153/Chop10. *Mol. Cell. Biol.* **16**, 1157–1168 (1996).
18. Su, N. & Kilberg, M.S. C/EBP homology protein (CHOP) interacts with activating transcription factor 4 (ATF4) and negatively regulates the stress-dependent induction of the asparagine synthetase gene. *J. Biol. Chem.* **283**, 35106–35117 (2008).
19. Wang, X.Z. & Ron, D. Stress-induced phosphorylation and activation of the transcription factor CHOP (GADD153) by p38 MAP kinase. *Science* **272**, 1347–1349 (1996).
20. Ubeda, M. & Habener, J.F. CHOP transcription factor phosphorylation by casein kinase 2 inhibits transcriptional activation. *J. Biol. Chem.* **278**, 40514–40520 (2003).
21. Wang, X.Z. *et al.* Identification of novel stress-induced genes downstream of chop. *EMBO J.* **17**, 3619–3630 (1998).
22. McCullough, K.D., Martindale, J.L., Klotz, L.O., Aw, T.Y. & Holbrook, N.J. Gadd153 sensitizes cells to endoplasmic reticulum stress by down-regulating Bcl2 and perturbing the cellular redox state. *Mol. Cell. Biol.* **21**, 1249–1259 (2001).
23. Ishikawa, F. *et al.* Gene expression profiling identifies a role for CHOP during inhibition of the mitochondrial respiratory chain. *J. Biochem.* **146**, 123–132 (2009).
24. Ohoka, N., Yoshii, S., Hattori, T., Onozaki, K. & Hayashi, H. TRB3, a novel ER stress-inducible gene, is induced via ATF4-CHOP pathway and is involved in cell death. *EMBO J.* **24**, 1243–1255 (2005).
25. Marciniak, S.J. *et al.* CHOP induces death by promoting protein synthesis and oxidation in the stressed endoplasmic reticulum. *Genes Dev.* **18**, 3066–3077 (2004).
26. Puthalakath, H. *et al.* ER stress triggers apoptosis by activating BH3-only protein Bim. *Cell* **129**, 1337–1349 (2007).
27. Namba, T. *et al.* Positive role of CCAAT/enhancer-binding protein homologous protein, a transcription factor involved in the endoplasmic reticulum stress response in the development of colitis. *Am. J. Pathol.* **174**, 1786–1798 (2009).
28. Treton, X. *et al.* Altered endoplasmic reticulum stress affects translation in inactive colon tissue from patients with ulcerative colitis. *Gastroenterology* **141**, 1024–1035 (2011).
29. Sturm, A. & Dignass, A.U. Epithelial restitution and wound healing in inflammatory bowel disease. *World J. Gastroenterol.* **14**, 348–353 (2008).
30. Iwata, Y. *et al.* CD19, a response regulator of B lymphocytes, regulates wound healing through hyaluronan-induced TLR4 signaling. *Am. J. Pathol.* **175**, 649–660 (2009).
31. Heijmans, J. *et al.* ER stress causes rapid loss of intestinal epithelial stemness through activation of the unfolded protein response. *Cell Rep.* **3**, 1128–1139 (2013).
32. Zinszner, H. *et al.* CHOP is implicated in programmed cell death in response to impaired function of the endoplasmic reticulum. *Genes Dev.* **12**, 982–995 (1998).
33. Jauhiainen, A. *et al.* Distinct cytoplasmic and nuclear functions of the stress induced protein DDIT3/CHOP/GADD153. *PLoS One* **7**, e33208 (2012).
34. Barone, M.V., Crozat, A., Tabaee, A., Philipson, L. & Ron, D. CHOP (GADD153) and its oncogenic variant, TLS-CHOP, have opposing effects on the induction of G1/S arrest. *Genes Dev.* **8**, 453–464 (1994).
35. Tsukano, H. *et al.* The endoplasmic reticulum stress-C/EBP homologous protein pathway-mediated apoptosis in macrophages contributes to the instability of atherosclerotic plaques. *Arterioscler. Thromb. Vasc. Biol.* **30**, 1925–1932 (2010).
36. Kojima, E. *et al.* The function of GADD34 is a recovery from a shutoff of protein synthesis induced by ER stress: elucidation by GADD34-deficient mice. *FASEB J.* **17**, 1573–1575 (2003).

37. Iizuka, M. & Konno, S. Wound healing of intestinal epithelial cells. *World J. Gastroenterol.* **17**, 2161–2171 (2011).
38. Araki, Y., Mukaisyo, K., Sugihara, H., Fujiyama, Y. & Hattori, T. Increased apoptosis and decreased proliferation of colonic epithelium in dextran sulfate sodium-induced colitis in mice. *Oncol. Rep.* **24**, 869–874 (2010).
39. Owen, C.R., Yuan, L. & Basson, M.D. Smad3 knockout mice exhibit impaired intestinal mucosal healing. *Lab. Invest.* **88**, 1101–1109 (2008).
40. Pickert, G. *et al.* STAT3 links IL-22 signaling in intestinal epithelial cells to mucosal wound healing. *J. Exp. Med.* **206**, 1465–1472 (2009).
41. Owen, K.A., Abshire, M.Y., Tilghman, R.W., Casanova, J.E. & Bouton, A.H. FAK regulates intestinal epithelial cell survival and proliferation during mucosal wound healing. *PLoS One* **6**, e23123 (2011).
42. Horndasch, M. *et al.* The C/EBP homologous protein CHOP (GADD153) is an inhibitor of Wnt/TCF signals. *Oncogene* **25**, 3397–3407 (2006).
43. Arai, N., Mitomi, H., Ohtani, Y., Igarashi, M., Kakita, A. & Okayasu, I. Enhanced epithelial cell turnover associated with p53 accumulation and high p21WAF1/CIP1 expression in ulcerative colitis. *Mod. Pathol.* **12**, 604–611 (1999).
44. Sipos, F., Molnar, B., Zagoni, T., Berczi, L. & Tulassay, Z. Growth in epithelial cell proliferation and apoptosis correlates specifically to the inflammation activity of inflammatory bowel diseases: ulcerative colitis shows specific p53- and EGFR expression alterations. *Dis. Colon Rectum* **48**, 775–786 (2005).
45. Munkholm, P. Review article: the incidence and prevalence of colorectal cancer in inflammatory bowel disease. *Aliment. Pharmacol. Ther.* **18** (Suppl 2), 1–5 (2003).
46. el Marjou, F. *et al.* Tissue-specific and inducible Cre-mediated recombination in the gut epithelium. *Genesis* **39**, 186–193 (2004).
47. Katakura, K., Lee, J., Rachmilewitz, D., Li, G., Eckmann, L. & Raz, E. Toll-like receptor 9-induced type I IFN protects mice from experimental colitis. *J. Clin. Invest.* **115**, 695–702 (2005).
48. Rath, H.C. *et al.* Normal luminal bacteria, especially Bacteroides species, mediate chronic colitis, gastritis, and arthritis in HLA-B27/human beta2 microglobulin transgenic rats. *J. Clin. Invest.* **98**, 945–953 (1996).
49. Neurath, M.F. *et al.* Assessment of tumor development and wound healing using endoscopic techniques in mice. *Gastroenterology* **139**, 1837. e1–1843.e1 (2010).
50. Whitehead, R.H. & Robinson, P.S. Establishment of conditionally immortalized epithelial cell lines from the intestinal tissue of adult normal and transgenic mice. *Am. J. Physiol. Gastrointest. Liver Physiol.* **296**, G455–G460 (2009).